Evaporation and quantum tunneling of electrons from a helium surface

J. M. Goodkind, Gordon F. Saville, and Andrei Ruckenstein
Physics Department, University of California at San Diego, La Jolla, California 92093

P. M. Platzman
AT&T Bell Laboratories, Murray Hill, New Jersey 07974

(Received 22 January 1988)

We have measured the escape rate of electrons from two-dimensional surface states of bulk helium. These measurements were made through a range of densities, external field, and temperature where thermal activation dominates ($T \geq 0.6$ K) into the range where quantum tunneling dominates ($T \leq 0.6$ K). Both processes are sensitive to electron-electron correlation effects. The thermal activation rates depend only on the barrier height for which a relatively simple approximation of the correlation is adequate. However, observed tunneling rates are many orders of magnitude greater than would be predicted by this same approximation.

INTRODUCTION

Evaporation and tunneling from a well-characterized, quantum-mechanical, many-particle system are processes that have a bearing on a variety of real physical systems.[1] A theoretical description of these processes requires a solution of many, seemingly simple, quantum-mechanical many-body problems which, nonetheless, cannot easily be solved by perturbation theory[2,3] or the use of classical concepts. The influence of dissipation (phonons) on the tunneling is an example.[4]

Very little progress has been made, although some work has been done on simplified models. Extensive analysis of simple two-level systems with linear coupling to a heat bath has revealed the great difficulty of the problem.[4] Simplified model potentials for other systems have been considered and a number of papers utilizing Wentzel-Kramers-Brillouin–type (WKB) methods have appeared.[5]

On the experimental side, there have been numerous investigations of a variety of physical systems including heterojunction tunneling,[6,1] tunneling through metal-insulator-metal junctions,[7,1] p-n tunnel diodes,[8,1] and Josephson junctions.[9,1] For such systems it is difficult to specify precisely, or to change systematically, the variables which govern the tunneling. In this paper we present measurements of evaporation and tunneling of electrons from the two-dimensional (2D) electron liquid formed on the surface of liquid helium at temperatures near 0.5 K. In contrast to the other systems, this one is unusual in several ways:

(1) It is extraordinarily clean in that it is free of the defects and impurities which complicate experiments in the other systems.

(2) The interaction Hamiltonian which fully describes all of the microscopic detail of the system is known. It consists of the coupling to the helium substrate, the Coulomb coupling to other electrons in the plane, and the external applied electric field. This system is an almost perfect physical realization of a quasi-2D liquid coupled to a background of excitations (ripplons).

(3) The fields required to produce tunneling are very modest (tens of volts/cm).

Although a previous experiment studied the escape rates in this system, it was performed at higher temperatures where only very rapid thermally activated escape over the barrier induced by sudden reversal of the external electric field could be observed.[10] In this work we have measured slow escape rates (10^{-5}–10^{-3} per electron per second) in both the tunneling and the thermally activated regimes. We will show that the simplest theory, using a one-particle potential, is in serious disagreement with the experimental results for tunneling. We make some general suggestions regarding a correct theory of this tunneling process.

THE PHYSICAL SYSTEM

The system we are investigating consists of an approximately uniform layer of electrons at density $n \cong 10^8/\text{cm}^2$ on the surface of bulk liquid helium at a temperature $\cong 0.5$ K. An external, variable, "pressing field," E_p, normal to the surface, is used initially to force the electrons onto the surface. Later, electrons are allowed to escape by reducing E_p. Near the surface of the liquid the electrons are attracted by an image potential of the form

$$V(z)=\begin{cases} -\Lambda_0 e^2/z\ , & 0<z<\infty \\ V_0\ , & z<0\ . \end{cases} \tag{1}$$

The squared "effective charge" for the ^{4}He-vacuum interface is

$$\Lambda_0=(\epsilon_1-1)/4(\epsilon_1+1)\cong 0.01\ , \tag{2}$$

where $\epsilon_1 \cong 1.05$ is the dielectric constant of liquid helium. The negative of the electron affinity $V_0 \sim 1$ eV is the energy required to force an electron into the liquid, assuming no bubbles are formed. The bound states of the electrons thus have a hydrogenlike spectrum,

$$E_N = -E_R/N^2 \ (N=1,2,\ldots,) \ .$$

The corresponding Rydberg energy $E_R = \Lambda_0^2 me^4/2\hbar^2$ is of order 10 K and the Bohr radius $a_B = \hbar^2/\Lambda_0 me^2$ is of order 100 Å.

Thus, the electron potential has three terms for $z > 0$:

$$U_B(z) = V(z) + |e| E_p z + V_c(z) \ . \tag{3}$$

$V_c(z)$ is the potential due to other electrons on the surface so that if there were no correlation among the electrons, the charge would be uniformly distributed on the surface and

$$V_c^0(z) = -2\pi ne^2 z \ . \tag{4}$$

However, there are two reasons why $V_c^0(z)$ fails to describe the system. Since the ratio of the electrostatic potential energy to the thermal energy is large,

$$\Gamma = (\pi n)^{1/2} e^2/k_B T \cong 100 \ , \tag{5}$$

there are strong correlations among the electrons.[11] In addition, the tunneling process cannot be correctly described by any static potential. As an electron tunnels from the surface the remaining electrons rearrange themselves. With these limitations in mind we use the preceding potential to estimate the magnitude of some of the physically important parameters of the system.

When the surface is "fully charged" $E_p = 2\pi n|e|$, but in order to allow electrons to escape, E_p is reduced such that $E_p = \delta 2\pi n|e|$ with $\delta < 1$. Then, in terms of Eq. (4), Eq. (3) becomes

$$U_B^0(z) = -\Lambda_0 e^2/z - (1-\delta) z (2\pi ne^2) \ . \tag{6}$$

The maximum in this potential occurs at

$$z_{\max}^0 = a_B(\epsilon)^{-1/2}$$

and

$$U_{B_{\max}}^0 = -4\pi ne^2(1-\delta)\epsilon^{-1/2} a_B \ ,$$

where

$$\epsilon = (1-\delta)2\pi n a_B^2/\Lambda_0 \ll 1$$

(see Fig. 1). If this, or any other one-particle potential correctly described the system, then at high temperatures one would observe an activated rate of charge loss,

$$W \sim \exp\{-[U_B(z_{\max}) - E_1]/k_B T\} \ . \tag{7}$$

At low temperatures there would be a temperature-independent tunneling rate given approximately by the WKB formula ($\hbar = 1$, and all rates in $\sec^{-1}$),

$$W \cong (E_1/2)\exp\left[-2\int_{z_1}^{z_2} \sqrt{2m[U_B(z) - E_1]}\, dz\right] \ . \tag{8}$$

The limits of integration are those values of z where the potential energy $U_B(z) = E_1$. For the potential in Eq. (6), $z_1 \cong 2a_B$ and $z_2 \cong a_B/2\epsilon$. For $U_B(z) - E_1 \cong 10$ K,

$$\sqrt{2m[U_B(z) - E_1]} \cong 1.5 \times 10^6 \ \text{cm}^{-1} \ .$$

There are a number of ways in which one could attempt to account for the electron correlations by simple static approximations. Iye *et al.*[10] did this by assuming that when an electron is in the plane, the other electrons are excluded from a disc surrounding it of radius r_0. For $\Gamma > 50$, $r_0 \cong 1.38(\pi n)^{-1/2}$. As the electron moves upward the hole shrinks and disappears when $z = r_0$. The authors compute this potential as a function of z using a number of plausible assumptions and find (see Fig. 1)

$$V_c^I(z) = -2\pi ne^2(z^2/2r_0) \ , \quad z < r_0 \ ,$$

$$V_c^I(z) = -2\pi ne^2(z - r_0/2) \ , \quad z > r_0 \ . \tag{9}$$

This reduces the contribution from the charge sheet so that the potential barrier is higher,

$$U_B^I(z_{\max}) = \pi ne^2 r_0 \delta^2 \ , \tag{10}$$

and wider,

$$z_2 = [a_B/\epsilon + r_0/(1-\delta)]/2 \ , \tag{11}$$

for $\delta > 0.5$.

If, on the other hand, we think of the tunneling as an instantaneous process, we can think of the charge distribution as being "frozen" in place during the tunneling process. In this case

$$V_c^F(z) = -2\pi ne^2[(r_0^2 + z^2)^{1/2} - r_0] \ , \tag{12}$$

and the barrier is even higher and wider (see Fig. 1).

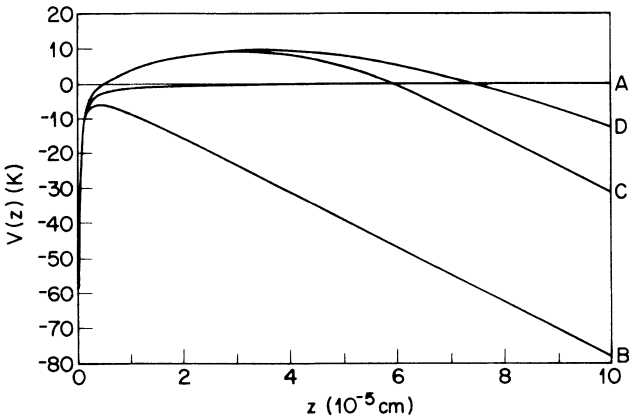

FIG. 1. Potential of an electron as a function of position, z, above the surface of the liquid helium. Curve A is the hydrogenic potential alone with $\delta = 1$. The remainder of the curves are for $\delta = 0.45$ and $n = 1.35 \times 10^8$ cm^{-2}. B is the potential in the presence of a uniform charge distribution (without any "correlation hole"), C is with the correlation hole as used by Iye *et al.*, and D is for the "frozen" hole in the charge distribution.

EXPERIMENTAL TECHNIQUE

Sample cell

The experimental cell (Fig. 2) has two horizontal parallel capacitor plates 2 cm in diameter, separated by 1 cm. The upper plate has a small hole through its center. A

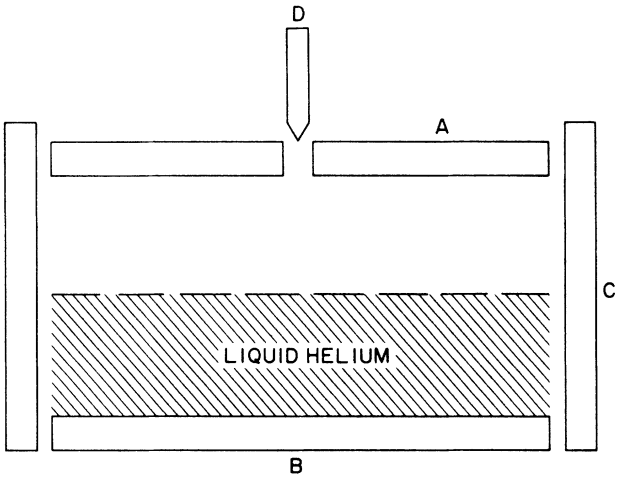

FIG. 2. Diagram (cross section) of the cylindrical experimental sample container. A is the upper capacitor plate, B is lower plate, C is the ring plate that provides the radial containing field, and D is the point of discharge for generating free electrons.

point electrode located just above this hole is charged to about -400 V to initiate a discharge. The discharge is performed at a temperature of about 0.98 K where the gas pressure is sufficient to sustain the discharge. The bottom plate is held at dc ground potential. During the discharge the (negative) potential of the upper plate, V_p, is gradually decreased so as to provide the pressing field that forces the electrons onto the surface. Values of V_p ranging between -15 and -300 V have been used.

The space between the plates is filled approximately half way with liquid helium. A cylinder surrounding the plates, but insulated from them, is held at a negative potential, V_r, so as to provide a radial field to prevent the electrons from reaching the walls of the container. In this geometry the charge forms a circular disc with maximum density, n_0, at its center. The diameter of the disc depends on V_p, V_r, and the total charge, Q, as described later. The electrons move in the plane of the liquid surface in response to the horizontal components of the ac field used to measure the capacitance. If the diameter of the charge disc is close to that of the retaining cylinder, the capacitance between the plates is substantially reduced by the shielding effect of the electron layer. As the diameter of the disc decreases, its shielding effect decreases so that the capacitance between plates increases. Thus the capacitance can be used as a measure of the disc diameter and, consequently, of the total charge on the surface.

The capacitance is measured using a 1 kHz drive signal with amplitude of 0.5 V. The detector is a General Radio capacitance bridge with a lock-in amplifier. In order to be certain that the bridge drive does not heat the electrons, measurements were repeated at higher and lower drive voltages at several temperatures. Anomalous behavior was observed at 2 V drive but 0.5 V was well below the level where the problem could be observed. The initial reading of the capacitance bridge, before depositing the charge, was about 0.401 00 pF. This was reduced to as low a value as 0.3100 pF by the charge, but the working range has normally been between 0.380 00 and 0.400 00 pF. The resolution of the measurements was 0.000 02 pF.

With no charge on the surface of the helium, the capacitance between the top and bottom plate is $C=-dQ_B^0/dV_p$, where Q_B^0 is the charge on the bottom plate resulting from the applied voltages V_p and V_r. When charge Q is present on the surface of the helium, an additional (image) charge, Q_b, is induced on the bottom plate. Its value depends only on the distribution of Q over the surface and the level, d, of the surface. The capacitance then becomes

$$C=-dQ_B^0/dV_p-(\partial Q_b/\partial V_p)_Q\ ,$$

so that the difference between capacitance with and without charge on the helium surface is

$$\Delta C=-(\partial Q_b/\partial V_p)_Q\ . \tag{13}$$

The quantitative determination of the total charge, as well as the charge distribution over the surface and the electric fields on the surface, requires numerical computation. A computer code similar to one used by Lambert and Richards[12,13] is used.

The code is run several times to give tables of $\Delta C(V_p,V_r,R,d)$, $Q(V_p,V_r,R,d)$, and $n_0(V_p,V_r,R,d)$, where R is the radius of the charge disk. It also gives the complete density profile as a function of radius r. Typical examples are shown in Fig. 3. Inverting these tables gives the more useful forms of $Q(\Delta C,V_p,V_r,d)$ and $n_0(\Delta C,V_p,V_r,d)$. In all of the preceding computations we neglected the small dielectric constant of the liquid helium, tilt of the sample cell, and deviations of the sample cell from ideal geometry. We estimate the total error from these approximations plus numerical errors in the computation to be less than 5%.

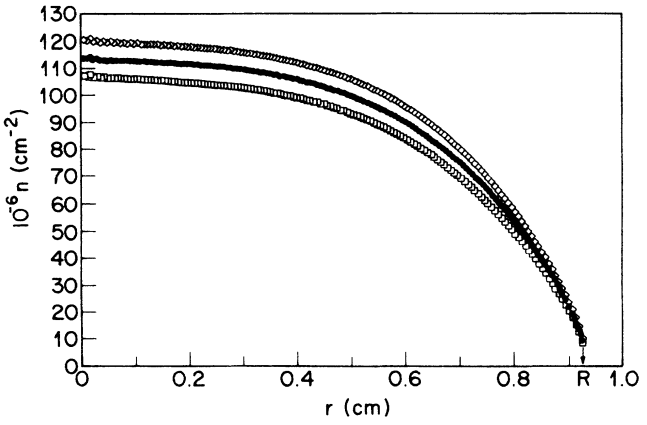

FIG. 3. A typical density profile for three different values of the pressing voltage V_p, in V; □, $V_p=-80$; ●, $V_p=-75$; and ◇, $V_p=-70$. In all cases the radial potential $V_r=-97$.

The results are strongly dependent on the helium level, d. Since our level sensing capacitor was unfortunately not working during the run, the code was also used to determine the level (which was not changed during the entire run). This was done by measuring ΔC for various values of V_p but fixed V_r and fixed, but initially unknown, Q in a regime where $|V_p| > V_c$, a critical voltage above which no charge escapes and the radius is a reversible function of V_p. Since Q was constant, the calculated $Q(\Delta C, V_p, V_r, d)$ should also be constant if the correct d is input. Thus, by stipulating constant Q and using measured values of ΔC, V_p, and V_r, the helium level d was determined to be approximately 0.44 cm.

In principle, the code allows us to compute the vertical component of the electric field, E_p, at the center of the charge pool. In practice we have adopted an approximate procedure. The code computes the contribution to E_p from the external potentials. We then approximate the contribution from the induced image charge on the top and bottom plates by assuming that Q_b covers the bottom plate uniformly so that the density is $n_b = Q_b / eA_{\text{plate}}$, and that the plates are infinite and parallel. The corresponding charge on the top plate is then $n_t = n_b[d/(D-d)]$ (where $D = 1$ cm is the spacing between plates) and the field from both charge densities is $2\pi(n_b - n_t)|e|$. Our stated values of E_p include this field. Although this is a crude estimate, the contribution to the total field is always less than 10% so that we have no need for greater precision.

Thermometry

The primary thermometer was the vapor pressure of ^{3}He contained in a separate chamber. It was used to calibrate a germanium resistance thermometer.

Procedure

After charging the surface, the system is cooled to the desired starting temperature. Then V_p is reduced in steps until a small but measurable escape rate is observed. The temperature is then raised in steps. The rate of change of the capacitance bridge output is determined from the raw data by linear regression to the data between steps in V_p or T. Figure 4 is an example of the output signal from the capacitance bridge. It shows both the stepwise, reversible changes due to reductions of V_p and the changes in slope that measure the escape rates.

DESCRIPTION OF RESULTS

Activation energy

Figure 5 shows the results of a series of measurements on a single charge pool. The escape rate (per electron) is shown as a function of temperature starting at temperatures below 0.5 K. Initially there is little or no temperature dependence. We have interpreted this to be the quantum tunneling regime. At higher temperatures the escape rate approaches an exponential dependence, characteristic of thermal activation over a barrier. When the temperature was well into the region of thermal activation, the pressing field was temporarily increased to stop the escape and the system was again cooled down below 0.5 K. Subsequently, the field was decreased again so as to allow a tunneling rate comparable to that of the previous data sets. The temperature was then increased to measure a new curve. On each successive warm up, the total charge was smaller. Consequently, $|V_p|$ is reduced so as to obtain comparable escape rates on all data series.[14]

The solid lines in Fig. 5 are fits to the data of functions

$$W = A[B\exp(-E_B^I/T)+1]\,. \tag{14}$$

A represents the tunneling rate (per electron), B the ratio of thermal activation rate to tunneling rate, and E_B^I is the computed activation energy using the simple model of Iye *et al.*, i.e.,

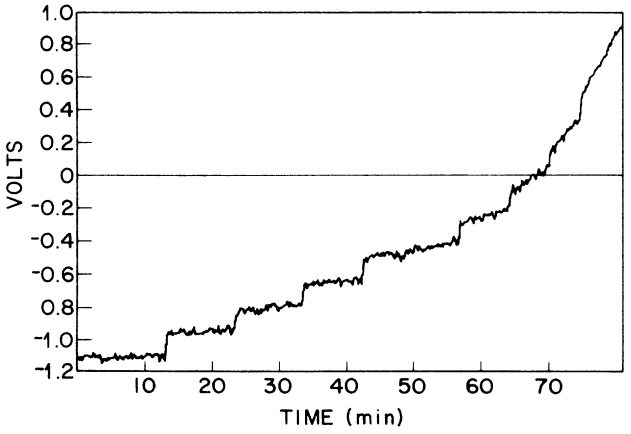

FIG. 4. The capacitance bridge output as a function of time showing the reversible changes (steps) due to reductions of V_p and the drifts due to escaping electrons. The escape rates increase as the pressing field is reduced.

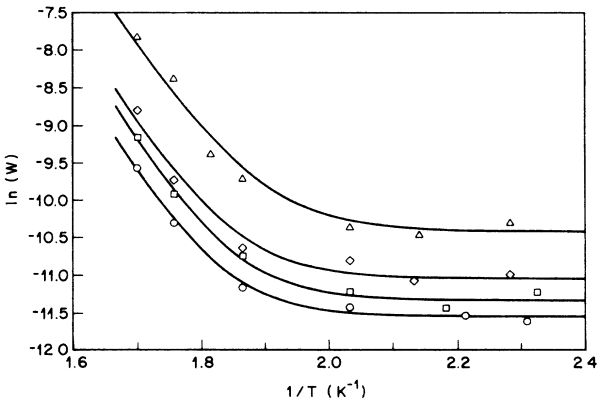

FIG. 5. The log of the escape rate vs $1/T$ at approximately constant charge. The solid lines represent the function in Eq. (14). The values of the parameters are shown in Table I. The curves are for four different values of the pressing voltage V_p in V; □, $V_p = -38$; ○, $V_p = -37$; ◇, $V_p = -34$; △, $V_p = -29.5$.

TABLE I. Values for the solid curves shown in Fig. 5. The parameters E_B^I, A and B are those of Eq. (14). V_p is the voltage on the top plate and n is the electron density.

V_p (V)	E_B^I (K)	A (10^5 sec^{-1})	$10^{-11}B$	range of n (10^8/cm^2)
−38.00	14.4	1.21	3.25	1.51–1.47
−36.99	14.4	0.971	2.60	1.45–1.43
−34.08	13.7	1.60	0.95	1.43–1.40
−29.50	12.8	2.99	0.32	1.40–1.34

$$E_B^I = U_B^I(z_{\max}) - E_1 \ .$$

These data are summarized in Table I.

The activation energy, E_B, is a function of two independent variables, E_p and n_0. Experimentally, E_B was determined by a linear regression of $\ln(W)$ versus $1/T$ (K^{-1}) in a regime where the escape rate W is dominated by thermal activation. For comparison the computed activation energy E_B^I, using the simplified model of Iye *et al.*, has been computed for the corresponding values of E_p and n_0. A complete listing of the data is presented in Table II. Agreement is generally good, indicating qualitative agreement with the static potential description of the thermal activation process.[15]

Tunneling

Measured tunneling rates are shown in Table III. The rates are a rapid function of the density and of E_p so that the data shown are for approximately constant n_0. Figure 6 shows the rate W ($W \equiv Q^{-1}dQ/dT$) as a function of the parameter $\delta = E_p/2\pi n\,|\,e\,|$. Over the narrow range of E_p, for which the tunneling was measurable, $\ln(W)$ is proportional to E_p. A linear regression to the data yields the following relations

$$\begin{aligned} \ln(W) &= -0.12E_p + 10.73 \ , \quad 4.54 > n_0 > 4.52 \ , \\ \ln(W) &= -0.141E_p + 2.70 \ , \quad 2.74 > n_0 > 2.73 \ , \\ \ln(W) &= -0.145E_p + 4.06 \ , \quad 1.44 > n_0 > 1.38 \ , \end{aligned} \tag{15}$$

when E_p is in V/cm and n_0 is in units of 10^8 cm^{-2}.

We have also computed tunneling rates by the WKB method using the same static potential used to compute the thermal activation energies in Table II. The ground-state energies used in these calculations incorporate first-order perturbation corrections due to the electric field term and $V_c(z)$ in Eq. (3). These results also obey a linear relation between $\ln(W)$ and E_p; however, the coefficient is 10 to 20 times larger than for the data. This means that the (negative) exponent in the calculated tunneling rate is about ten times larger than the measured value. Since the height of the barrier, as measured by the thermal activation, agrees with the theoretical potential, the width must be very much less than predicted. This is consistent with a dynamical readjustment of the charge on the surface into the position formerly occupied by the tunneling electron.

Some of the data in the tunneling regime indicate a slight decrease in tunneling rate with increasing tempera-

TABLE II. Measured and computed activation energies for various values of electric field, E_p, and charge density, n_0. Errors indicated are statistical errors computed from the linear regression to the data.

E_B (meas.) (K)	E_B^I (K)	E_p (V/cm)	n_0 (10^9/cm^2)	T_{average} (K)
24±0.2	24.1	70.2	0.123	0.955
23.1±0.5	22.4	69.9	0.131	0.965
14.7±0.4	17.5	31.3	0.058	0.73
14.3±0.3	16.5	25.6	0.048	0.73
14.6±0.4	16.1	21.1	0.038	0.73
17.8±0.5	17.6	58.0	0.133	0.67
17.4±1.5	17.1	58.4	0.139	0.64
15.9±0.3	16.2	55.0	0.136	0.615
12.9±0.8	15.5	53.6	0.139	0.595
15.8±0.8	15.4	52.0	0.134	0.615
14.6±0.3	14.6	48.5	0.130	0.63
14.8±0.3	13.9	48.0	0.138	0.575
15.2±0.2	16.6	43.1	0.095	0.695
15.9±1.2	16.1	39.4	0.088	0.655
10.5±0.	13.9	35.1	0.091	0.575
11.9±0.1	15.5	29.7	0.063	0.66
8.8±0.1	14.8	20.8	0.041	0.705
10.8±1.3	12.9	13.5	0.028	0.63

TABLE III. Measured tunneling rates for three different densities.

E_p (V/cm)	W (10^{-5}/sec)	n_o (10^9cm/^{2})
182.7	1.39	0.452
178.0	2.19	0.454
173.4	4.04	0.453
159.5	6.85	0.441
99.4	1.05	0.274
96.6	1.91	0.274
93.8	2.95	0.274
90.9	3.88	0.274
88.1	5.57	0.273
85.3	8.56	0.273
52.4	1.17	0.149
51.2	1.01	0.144
48.3	1.67	0.142
43.8	2.98	0.138
35.2	2.65	0.093

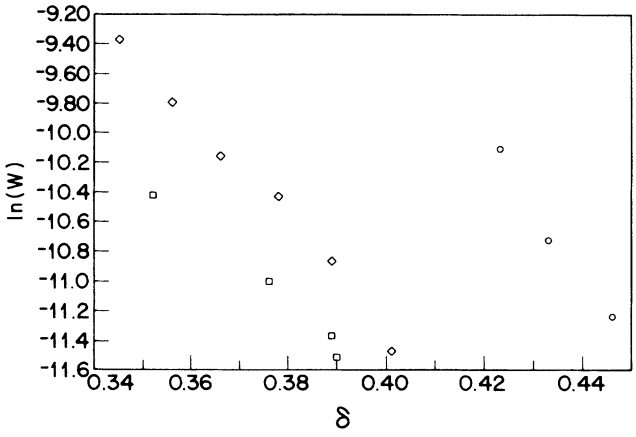

FIG. 6. Tunneling rate vs $\delta \equiv E_p/2\pi ne$ for three different densities: □, $n_0 = 1.49-1.38$; ◇, $n_0 = 2.74-2.73$; ○, $n_0 = 4.54-4.52$ (10^8 cm^{-2}).

ture. This can be seen in two of the curves in Fig. 5. Unfortunately, the data are not consistent in this regard so that more work is required to determine if it is truly a feature of the tunneling process. Some temperature dependence would be consistent with the coupling to ripplons, i.e., with the so-called "quantum dissipation" phenomenon.[2,4] The details of this interesting temperature dependence have not been worked out for our specific system.

Discussion of possible experimental artifacts and errors

The discharge method for obtaining free electrons has the disadvantage that electrons can land anywhere in the sample chamber including the helium film covering the sample walls. These electrons can then be effectively trapped by their image charge. Electrons arriving at the surface of the liquid with greater than 1 eV can penetrate the liquid and reach the plates. If plates have patches that are insulated by dirt or oxide, some of the electrons will remain on these patches and will alter the electric fields on the charge pool. If such charges were to move during a set of measurements, they would alter the observed time dependence of the capacitance. If the amount and distribution of such charge were different between successive measurements, it would contribute to the scatter of the results since the actual value of E_p would be different than computed from the known applied potentials. If the amount and distribution of such charge were highly reproducible it would result in a systematic error in E_p.

We expect that some of the random errors in the data result from random variations of the amount and distribution of stray charge. This is particularly true at low values of E_p. Future experiments designed to eliminate stray charge will test the possibility. Systematic errors that would alter the qualitative conclusions of this paper are ruled out by several arguments. The dependence of E_B on E_p is qualitatively and quantitatively consistent with the well-understood aspects of the potential as well as with previous experimental results.[10] Any stray charge in the system would alter both the thermally activated and tunneling escape rates in the same direction. Consequently, the fact that the tunneling rate is many times too large relative to the thermal escape rates would not be altered by the presence of stray charge.

If charge from the pool on the liquid surface were to escape along paths other than upward from the center of the pool, our interpretation of the results would be incorrect. The 1 eV barrier to penetration of the liquid makes escape through the liquid appear impossible. Escape along radial paths on the surface might occur when the edge of the pool is within a few microns of the ring plate. However, in our geometry, as $|V_p|$ is reduced in order to initiate the escape, the radius of the charge pool decreases. Thus, as our experiment proceeds ($|V_p|$ is reduced), escape along radial paths would decrease continuously, whereas the observed rate is constant until it begins to increase at a well-defined critical voltage.

The temperature-independent escape rate at low temperatures could, in principle, indicate simply that the electrons were not cooled below some limiting temperature. Several features of the data rule out this possibility. The most simply stated argument is based on the fact that the thermal transfer between the electrons and the helium proceeds via inelastic electron-ripplon scattering. This scattering rate[16] increases with increasing pressing field. Thus, the thermal contact would be best at the highest pressing fields so that the samples at high pressing fields would reach lower temperatures. On the other hand, the data show that the transition to the temperature-independent regime occurs at higher temperature for larger pressing fields.

Since the measured capacitance depends on the level of the liquid as well as the radius of the charge pool, variations of the liquid level will therefore appear as increases

or decreases of the amount of charge. In particular, we have observed small changes in capacitance when temperature differences between the ^{3}He pot and the ^{4}He pot are changed rapidly. We assume this results from a heat flush of superfluid ^{4}He into the filling capillary of the sample chamber. This could introduce a small artificial temperature dependence to the escape rates. However, measurements of capacitance versus time for constant $V_p(\,|\,V_p\,|\,>V_C)$ show that any contribution from this source is less than the scatter in the data.

CONCLUSIONS

The measured thermal activation energies are in reasonably good agreement with the simple, one-particle static potential used by Iye *et al.*, assuming the prefactor for the Arrhenius law exponential term is only weakly temperature dependent (i.e., not exponential). However, the observed tunneling rates are much too rapid for that potential. The "frozen" potential is even worse in this regard. On the other hand, the potential for a uniform charge distribution (no correlations) yields much more rapid tunneling than is observed. We do not have as yet a detailed microscopic description of this process, but the possibilities we are examining all focus on the dynamical nature of the tunneling process. Landauer and Buttiker (LB) showed in a very simple model using a potential modulated at frequency ω (Ref. 3) that a characteristic time enters the problem. $\tau_{LB}=L/v$, where L is the thickness of a square barrier and $v=\sqrt{2(U-E)/m}$ is the imaginary velocity under the barrier of height $(U-E)$. For $(U-E)\cong 10$ K and for $L\cong 10^{-4}$ cm, $\tau_{LB}\cong 5\times 10^{-11}$ sec. The typical response frequency of the 2D electron gas to the tunneling electron is the zone boundary plasmon $\omega^2=(2\pi ne^2/m)k$ with $k=\pi^{3/2}n^{1/2}$. For $n=10^8$ cm^{-2}, $\omega\tau_{LB}\cong 2$. In this case the tunneling electron may absorb energy from the electron gas as the gas overshoots to screen the hole left behind. This could lead to tunneling where the electron is boosted up in energy and emerges from the system at an energy higher than E_1. At these energies it has a smaller barrier to go through. It is also possible that in the process of tunneling the electron takes a path in the Feynman sense which is not along the z axis. In this case it takes advantage of the repulsive field of the neighboring electrons so that the effective potential for tunneling is closer to that of the uniform charge distribution than is the potential for thermal activation.

A successful theory of the tunneling process in this system should lead to a better understanding of the basic quantum tunneling process in the presence of coupling to other degrees of freedom. Good measurement of the weak temperature dependence in the tunneling regime should give us new insights into the effect of ripplonic degrees of freedom, "quantum dissipation," on quantum tunneling. Finally, it will be interesting to understand how a better theory preserves the agreement between the observed and statically calculated activation energies.

ACKNOWLEDGMENTS

We would like to thank A. Dahm and C. C. Grimes for several informative discussions. This research was partially supported by the National Science Foundation under Grant No. DMR-85-03832.

[1] *Tunneling in Solids,* edited by C. B. Duke (Academic, New York, 1969); J. Bardeen, Phys. Rev. Lett. **6**, 57 (1961); M. H. Cohen, L. M. Falicov, and J. C. Phillips, *ibid.* **8**, 316 (1962).

[2] A. J. Caldiera and A. J. Leggett, Phys. Rev. Lett. **46**, 211 (1981); T. R. Knowles and H. Suhl, *ibid.* **39**, 1417 (1977).

[3] M. Buttiker and R. Landauer, Phys. Rev. Lett. **49**, 1739 (1982); Phys. Scr. **32**, 429 (1987).

[4] A. J. Leggett, S. Chakavarty, A. T. Dorsey, M. P. A. Fisher, and A. G. W. Zwerger, Rev. Mod. Phys. **59**, 1 (1987).

[5] L. Landau and E. Lifshitz, *Quantum Mechanics* (Pergamon, New York, 1965); R. Bruinsma and P. Bak, Phys. Rev. Lett. **56**, 420 (1986).

[6] *18th International Conference on Semiconductors, Stockholm, Sweden, 1986,* edited by O. Engstrom (World Scientific, Singapore, 1987).

[7] M. Handy, Phys. Rev. **126**, 1968 (1962); I. Giaver, Phys. Rev. Lett. **5**, 147 (1960); **5**, 464 (1960).

[8] D. J. Dumin and G. L. Pearsen, J. Appl. Phys. **36**, 3410 (1965).

[9] C. B. Duke, in *Proceedings of the International Summer School on Electron Tunneling Phenomena in Solids* (Plenum, New York, 1969); B. D. Josephson, Adv. Phys. **14**, 419 (1969).

[10] Y. Iye, K. Kono, K. Kajita, and W. Sasaki, J. Low Temp. Phys. **38**, 293 (1980).

[11] H. Totsoji, Phys. Rev. A **17**, 399 (1978).

[12] D. K. Lambert and P. L. Richards, Phys. Rev. Lett. **44**, 1427 (1980).

[13] D. K. Lambert and P. L. Richards, Phys. Rev. B **33**, 3282 (1981).

[14] Runs were also made where V_p was held constant while the temperature was raised and lowered three times. The data show no systematic dependence on the direction of the temperature change.

[15] To measure the slope of the escape rate versus temperature, we have measured rates over a range of temperature ($\Delta T\cong 0.06$ K) and defined the temperature in the middle of the range as T_{average}.

[16] M. Saitoh, J. Phys. Soc. Jpn. **42**, 201 (1977); P. M. Platzman and G. Beni, Phys. Rev. Lett. **3671**, 626 (1976).